AFRL-AFOSR-JP-TR-2019-0020

Magnetically Doped Two Dimensional MoS2: Towards High Performance Spintronics Applications

Hui Ying Yang
Singapore University of Technology and Design

03/08/2019
Final Report

DISTRIBUTION A: Distribution approved for public release.

Air Force Research Laboratory
AF Office Of Scientific Research (AFOSR)/ IOA
Arlington, Virginia 22203
Air Force Materiel Command

REPORT DOCUMENTATION PAGE

Form Approved
OMB No. 0704-0188

The public reporting burden for this collection of information is estimated to average 1 hour per response, including the time for reviewing instructions, searching existing data sources, gathering and maintaining the data needed, and completing and reviewing the collection of information. Send comments regarding this burden estimate or any other aspect of this collection of information, including suggestions for reducing the burden, to Department of Defense, Executive Services, Directorate (0704-0188). Respondents should be aware that notwithstanding any other provision of law, no person shall be subject to any penalty for failing to comply with a collection of information if it does not display a currently valid OMB control number.
PLEASE DO NOT RETURN YOUR FORM TO THE ABOVE ORGANIZATION.

1. REPORT DATE *(DD-MM-YYYY)*	2. REPORT TYPE	3. DATES COVERED *(From - To)*
19-03-2019	Final	27 Aug 2015 to 26 Feb 2018

4. TITLE AND SUBTITLE
Magnetically Doped Two Dimensional MoS2: Towards High Performance Spintronics Applications

5a. CONTRACT NUMBER

5b. GRANT NUMBER
FA2386-15-1-4029

5c. PROGRAM ELEMENT NUMBER
61102F

6. AUTHOR(S)
Hui Ying Yang

5d. PROJECT NUMBER

5e. TASK NUMBER

5f. WORK UNIT NUMBER

7. PERFORMING ORGANIZATION NAME(S) AND ADDRESS(ES)
Singapore University of Technology and Design
287 GHIM MOH ROAD
Singapore, 279623 SG

8. PERFORMING ORGANIZATION REPORT NUMBER

9. SPONSORING/MONITORING AGENCY NAME(S) AND ADDRESS(ES)
AOARD
UNIT 45002
APO AP 96338-5002

10. SPONSOR/MONITOR'S ACRONYM(S)
AFRL/AFOSR IOA

11. SPONSOR/MONITOR'S REPORT NUMBER(S)
AFRL-AFOSR-JP-TR-2019-0020

12. DISTRIBUTION/AVAILABILITY STATEMENT
A DISTRIBUTION UNLIMITED: PB Public Release

13. SUPPLEMENTARY NOTES

14. ABSTRACT
Two dimensional (2D) transition metal dichalcogenides (TMDs) have received tremendous attention owing to its exceptional physical and chemical properties. Monolayer TMDs are direct bandgap semiconductors exhibiting strong photoluminescence (PL), excellent on/off current ratio, edge active relative catalysis, and spin-valleytronics needed for high-performance electronics. However, the yield of monolayer TMDs fabricated via mechanical exfoliation method is typically low, and not suitable for batch production. A chemical exfoliation approach provides better yield of monolayer TMDs, but it is still not a scalable technique with consistent yield.
For this work, a unique vertical chemical vapor deposition (CVD) method was developed to produce batch productions of molybdenum disulfide (MoS2) monolayer, a typical TMD material. Raman and PL mappings show the high quality of samples without defects at the edge sites; STEM and diffraction data show the high crystal quality. The electrical performance of CVD grown monolayer MoS2 by this technique is comparable to that of mechanically exfoliated samples. Although the common expectation that CVD grown MoS2 should be structurally defective due to thermal stresses during the growth process, the large mobility of samples achieved at 64 cm2/V-s (RT). Additionally, strong PL intensity is attributed to the p doping effects of adsorbates at the defect-sites of CVD samples and its PL intensities will decrease significantly when measured in vacuum. First principle calculations were carried out to investigate the charge transfer process between MoS2 and adsorbates and to further clarify the p-doping effect of adsorbates due to the strong electronegativity of adsorbates. Such a p-doping effect from adsorbates reduces the concentration of excess electron in MoS2 and contributes to the radiative process of excitons. All of this indicates th

15. SUBJECT TERMS
spintronics, magnetic, monolayer, superconducting, solid, material

16. SECURITY CLASSIFICATION OF:			17. LIMITATION OF ABSTRACT	18. NUMBER OF PAGES	19a. NAME OF RESPONSIBLE PERSON
a. REPORT	b. ABSTRACT	c. THIS PAGE			WINDER, SHEENA
Unclassified	Unclassified	Unclassified	SAR		19b. TELEPHONE NUMBER *(Include area code)* +81-42-511-2008

Standard Form 298 (Rev. 8/98)
Prescribed by ANSI Std. Z39.18

Magnetically Doped Two Dimensional MoS2: Towards High Performance Spintronics Applications

AFOSR Funding Project Report

Grant No. FA2386-15-1-4029

Associate Professor Yang Hui Ying

Singapore University of Technology and Design, Singapore

Project Motivation: Two dimensional (2D) transition metal dichalcogenides (TMDs) has received tremendous attention owing to its exceptional physical and chemical properties. Specifically, monolayer TMDs are direct bandgap semiconductors exhibiting strong photoluminescence (PL), excellent on/off current ratio, edge active relative catalysis, and spin-valleytronics. Nevertheless, the yield of monolayer TMDs fabricated via mechanical exfoliation method is typically low, and not suitable for batch production. Despite chemical exfoliation approach provides better yield of monolayer TMDs, it is still not a scalable technique with consistent yield. Hence, synthesis of large-area and high-performance monolayer TMDs is the most critical challenge for further development of TMDs as mainstream electronic materials.

Project Vision: This project's vision is to develop a novel, inexpensive and practical synthesis method for mass production of two dimensional nanomaterials for applications ranging from spintronics devices, optoelectronics device, and energy storage. This technique will make inexpensive volume production of 2D transition metal dichalcogenides monolayer, which will prompt great interests in both scientific research and commercialization in various applications.

Current Results Summary: Our team has developed a unique vertical chemical vapor deposition (CVD) method to produce batch productions of Molybdenum disulfide (MoS_2) monolayer, as a typical material in TMDs group. We have investigated the high crystal quality and explore their applications in optoelectronics devices, valleytronics devices and energy storage devices.

Research Achievements:

List of Publications under the support of AFOSR grant:

1. 'Recent Advances in Growth of Novel 2D Materials: Beyond Graphene and Transition Metal Dichalcogenides', Dechao Geng and **Hui Ying Yang**, Advanced Materials, 2018, 30, e1800865.
2. 'Concurrent Synthesis of High-Performance Monolayer Transition Metal Disulfides', Linfeng Sun, Wei Sun Leong, Shize Yang, Matthew F. Chisholm, Jing Kong and **Hui Ying Yang**, **Advanced Functional Materials**, 2017 issue.
3. 'Reversibly Tunable Photoluminescence in Chemical Vapor Deposited MoS2 by Charge Transfer with Active Adsorbates', L. F. Sun, X. Zhang, F. C. Liu, Y. D. Shen, X. F. Fan, S. J. Zheng, Z. Liu, H. J. Fan, S. A. Yang, H. Y. Yang, **Scientific reports**, 2018 issue.
4. 'Fe3O4 quantum dot decorated MoS2 nanosheet arrays on graphite paper as free-standing sodiumion battery anodes', Dezhi Kong, Chuanwei Cheng, Ye Wang, Zhixiang Huang, Bo Liu, Yew Von Lim, Qi Ge and **Hui Ying Yang**, **Journal of Materials Chemistry A**, 2017, 5, 9122.
5. 'Three-dimensional hierarchical NiCo2O4 Nanowires@Ni3S2 Nanosheets Core/Shell Arrays for Flexible Asymmetric Supercapacitor', B. Liu, D. Kong, Z. X. Huang, R. Mo, Y. Wang, Z. J. Han, C. Cheng, and H. Y. Yang, **Nanoscale**, 8, 10686, (2016).

DISTRIBUTION A: Approved for public release: distributuion unlimited

6. **Invited conference talk and paper** in 2016 IEEE International Conference on Electron Devices and Solid-State Circuits (**EDSSC 2016**).

Research Highlights

In our research supported by AFOSR funding, we have developed a very elegant technique to concurrently synthesize multiple monolayer transition metal disulphide films in the same furnace using the CVD approach. The process is to first disperse precursor powders (*e.g.* MoO_3 or WO_3) on the targeted Si/SiO_2 substrates followed by a sulfur annealing process to synthesize high-quality transition metal disulphide films (*e.g.* MoS_2 or WS_2). For instance, MoO_3 powders are dispersed on a group of targeted substrates for the synthesis of MoS_2 films while WO_3 powders are dispersed on another group of targeted substrates for the growth of WS_2 films. Using our proposed technique, substrates pre-coated with different precursors can be sulfur-annealed together in a CVD furnace to produce individual monolayer TMD films on separate substrates at the same time. More importantly, only MoS_2 films are grown on those substrates pre-coated with MoO_3 powders while only WS_2 films are grown on other substrates that were pre-coated with WO_3 powders. The monolayer MoS_2 (WS_2) samples were grown using MoO_3 (WO_3) and sulfur as precursors on a clean SiO_2/Si wafer with a 285 nm SiO_2 thickness. The experimental steps in our work are shown in **Figure 1**a-d. Here the description mainly focuses on the concurrent synthesis process. Firstly, the MoO_3 (WO_3) powder was deposited on the surface of SiO_2/Si wafer. The MoO_3 (WO_3) powder was distributed randomly on the surface of wafers by compressed nitrogen gas gun. Then they were put vertically in the pre-designed ceramic boat (as shown in Figure 1f), and finally monolayer MoS_2 (WS_2) samples could be observed by optical microscopy after the growth process. During the growth process, it was put at the center of the furnace. Another ceramic boat filled with sulfur powder was placed at the edge of the furnace as the lower melting point of sulfur (Figure 1e).[28, 29] It shows that the thickness distribution of boundary layer in our work is uniform, which maybe contribute to the uniform coverages of monolayer MoS_2 (WS_2) on SiO_2/Si substrate. During the growth process, the ceramic boat with S powder is very critical to the growth of monolayer MoS_2 (WS_2) as it is well known that the partial pressure of the precursors could affect the subsequent adsorption and the surface bound reaction on the substrate.[30] The excess of S could suppress the volatilization of MoO_3 (WO_3) and the reduced concentration of S may lead to the low-valence-state oxide or oxysulphide nanoparticles. We investigated the temperature range from 700°C to 850°C as the growth temperatures reported in literature are mainly in this range.[20, 31-33]

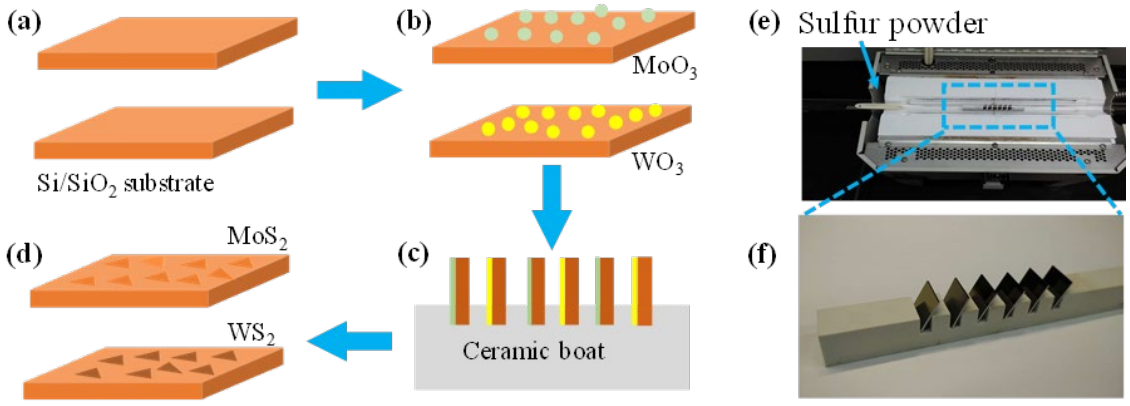

DISTRIBUTION A: Approved for public release: distributuion unlimited

Figure 1. a-d) show the schematic illustration of the designed experimental steps for concurrent growth of monolayer MoS_2 and WS_2 by CVD. e) The furnace used in the work. The position of ceramic boat with sulfur powder is controlled by a pairs of magnets. The one is inside and the other one is outside of the furnace. f) The picture of the fabricated ceramic boat used in experiment, with the SiO_2/Si substrate vertically put on it.

Figure 2a shows the optical image of CVD grown monolayer MoS_2 samples on SiO_2/Si substrate, which were obtained with a Nikon microscope. Other pictures are shown in Figure S5. From these optical images, we found the coverage of monolayer MoS_2 is relatively uniform, no matter the size and the distribution of triangular MoS_2. Figure 2b shows the enlarged figure and some clear monolayer MoS_2 with triangular shape could be observed with the average size ~20 µm. Figure 2c and 2d shows the Raman and PL spectra of the concurrent synthesis of monolayer MoS_2 and WS_2, respectively. The monolayer MoS_2 exhibits two prominent Raman peaks: E^1_{2g}, and A_{1g}, at 384.63cm^{-1} and 402.58 cm^{-1}, respectively. The frequency difference between the two prominent peaks is ~18 cm^{-1}, which is almost the same as that reported for mechanically exfoliated single layer MoS_2. The PL spectrum shows two typical emission peaks marked as A and B. The origin of these two peaks has been known as the optical transitions at K point because of the spin orbital splitting at the top of valence band.[3] The monolayer WS_2 also show its typical Raman modes, corresponding to the reported results when excited by 532nm laser line. One typical emission peak was also observed in Figure 2d. Figure 2e and 2f show the PL and Raman mapping of a typical CVD grown MoS_2 sample. The Raman mappings were normalized to the intensity of A_{1g} mode and the PL mapping was integrated by the intensity of A exciton emission peak. From the Raman and PL mapping, we can observe that the sample is uniform and no additional layer on it. The uniformity of intensity in PL mapping indicates the high quality of sample without the structural defects or disorder at the edge of sample.

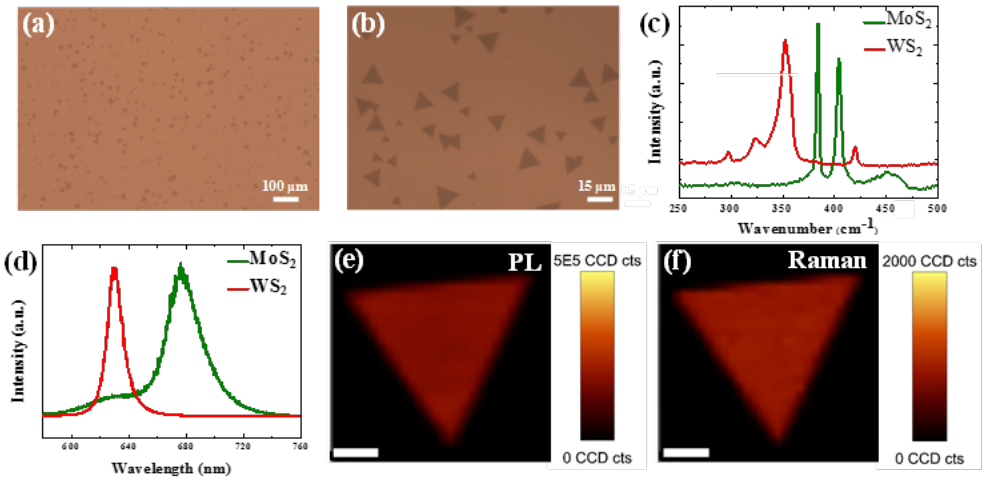

Figure 2. a) Optical images of CVD grown monolayer MoS_2 on SiO_2/Si substrate. The scale bar represents 100 µm. b) Optical image of several typical monolayer MoS_2 with triangular shape. Scale bar: 15µm. c) Raman and d) PL spectra of the concurrent synthesis of monolayer MoS_2 and WS_2, respectively. e,f) show the PL and Raman mapping of monolayer MoS_2, respectively. The scale bars represent are 2 µm.

DISTRIBUTION A: Approved for public release: distributuion unlimited

Our monolayer MoS_2 films exhibit high electrical performance comparable to those seen in exfoliated samples. Figure 3a shows the schematic of a back-gated MoS_2 field-effect transistor used in this work. More than 100 field-effect transistors fabricated on our monolayer MoS_2 films have been tested (see Experimental section for fabrication details). All our electrical measurements were performed in high vacuum at room temperature except for the temperature dependence study shown in Figure 3d. No annealing was performed on all our devices prior to electrical measurement. Figures 3b-c plot the output (I_D-V_D) and transfer (I_D-V_G) characteristics of a typical back-gated transistor fabricated on our CVD MoS_2 films, respectively. As can be seen, our MoS_2 transistor exhibits high on-current (49 mA/mm) at V_{DS} = 2 V and V_G = 50 V (Figure 4b) and n-type FET behavior with on-off ratio of 10^7 (inset of Figure 4c). We then extract the extrinsic mobility of this MoS_2 FET using equation (1):

$$\mu = \frac{1}{C_{ox} \bullet V_{DS}} \bullet \frac{L_{ch}}{W_{ch}} \bullet \frac{\Delta I_{DS}}{\Delta V_G} \qquad (1)$$

where C_{ox} is the gate capacitance (1.21×10^{-8} F/cm^2 for 285 nm thick SiO_2), L_{ch} and W_{ch} are channel length and width, respectively, I_{DS} is the drain current, V_{DS} is the drain voltage and V_G is the gate voltage. The electron mobility for the typical MoS_2 device is 64 cm^2/V-s, which to the best of our knowledge, is the highest value reported to date, for CVD grown MoS_2 films that were synthesized on Si/SiO_2 substrates, without any treatment.

DISTRIBUTION A: Approved for public release: distributuion unlimited

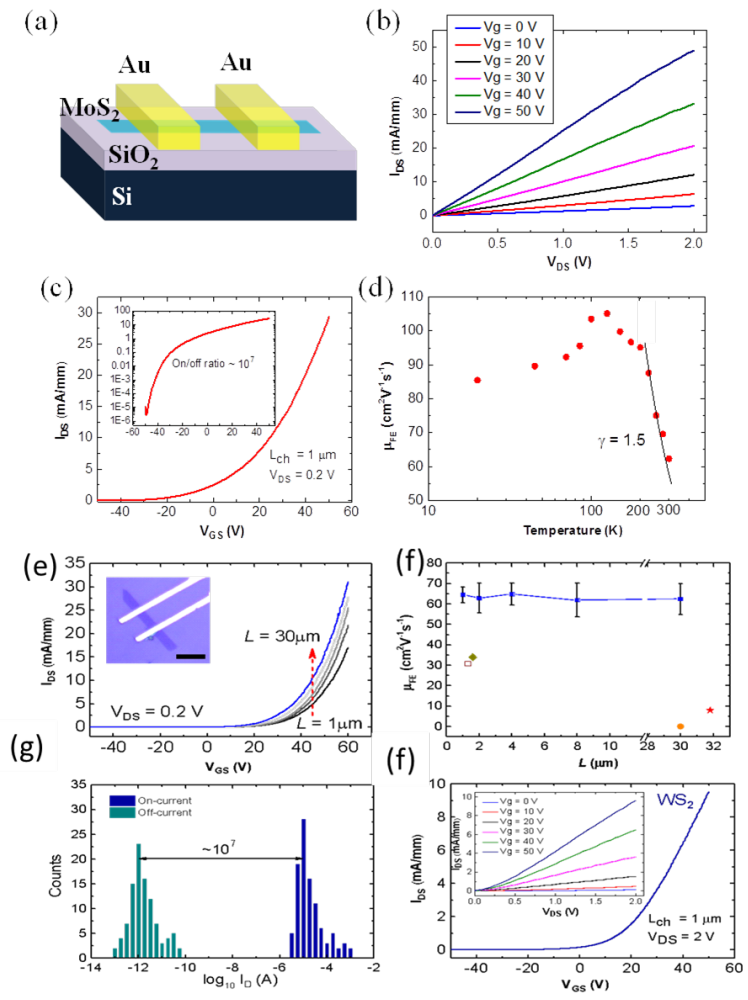

Figure 3. a) Schematic showing a back-gated MoS_2 field-effect transistor used in this work. b) I_D-V_D characteristics of a typical back-gated transistor fabricated on our CVD MoS_2 film. c) I_D-V_G characteristics of a typical back-gated transistor fabricated on our CVD MoS_2 film. The device's mobility is as high as 64 cm^2/V-s at room temperature. Inset: I_D-V_G characteristics of the same MoS_2 transistor in logarithmic scale. d) Temperature dependence of field-effect mobility, μ_{FE} measured from the same transistor showing phonon-limited intrinsic transport. e) I_D-V_G characteristics of five typical transistors fabricated on our CVD MoS_2 film with different channel lengths, *L* (1, 2, 4, 8 and 30 μm). Inset: Optical image showing a typical back-gated MoS_2 transistor with *L* = 8 μm. Scale bar: 10 μm. f) Average μ_{FE} measured from 100 MoS_2 transistors (blue squares) fabricated on random substrates with different *L*. The maximum μ_{FE} reported for CVD-grown MoS_2 (diamond, circle and star) and exfoliated MoS_2 samples (hollow square) are included for comparison purposes.[19, 34-36] g) Histogram of on-state and off-state current of 100 back-gated MoS_2 transistors showing a median on–off ratio of 10^7 and a high on-state current. h) I_D-V_G characteristics of a typical back-gated transistor fabricated on our CVD WS_2 film. The device's mobility is about 21 cm^2/V-s at room temperature. All electrical measurements were conducted at room temperatures except those in d.

In Figure 3d, the temperature dependence of field-effect mobility, μ_{FE} measured from the same

DISTRIBUTION A: Approved for public release: distributuion unlimited

transistor is plotted showing phonon-limited transport, similar to the behaviors previously observed in exfoliated MoS_2 samples. In addition, we have fabricated and tested transistors with different channel length, *L* (1, 2, 4, 8 and 30 μm) and we observed that our MoS_2 films consistently exhibit high electrical performance regardless of the channel length (Figures 3e). In Figure 3f, the average μ_{FE} measured from 100 MoS_2 transistors (blue squares) fabricated on random substrates with different channel length is plotted. For comparison purposes, we have included the maximum μ_{FE} reported for CVD-grown MoS_2 and exfoliated MoS_2 samples. As can be seen, transistors fabricated on our CVD MoS_2 samples exhibit mobility as least twice better than previous works. Figure 3g shows the histogram of on-state and off-state current of our 100 back-gated MoS_2 transistors showing a median on–off ratio of 10^7 and a high on-state current. Apart from that, more than 20 transistors have been fabricated on our monolayer WS_2 films and a typical I_D-V_G characteristic of our back-gated WS_2 transistors is plotted in Figure 3h.

In our project, by investigating the PL intensities of specifically defect-rich monolayer (1L) MoS_2 samples with the different fabrication methods, we aim to uncover the most likely emission mechanism to the strong PL in CVD MoS2 samples. First, the more defects (S vacancy) in CVD samples than that in ME samples is confirmed using energy dispersive spectroscopy (EDS) spectra. The vacuum level dependent PL intensities of CVD samples reveal the surface adsorbates may contribute to its strong PL.

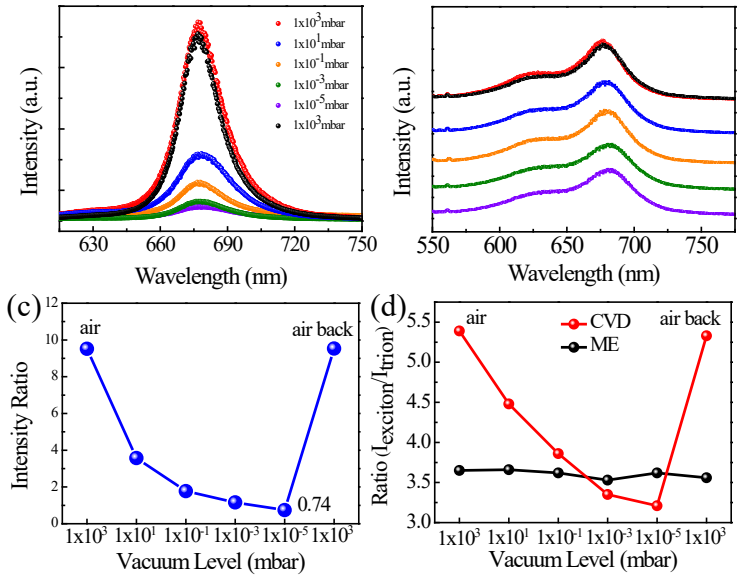

Figure 4. Vacuum level dependent PL spectra of CVD grown (a) and ME (b) MoS_2 samples. (c) The ratio of PL intensities between CVD grown and ME MoS_2 samples at different vacuum levels, shown in Figure (a) and (b). (d) Vacuum level dependence of the intensity ratios of exciton to trion emissions in CVD grown and ME samples.

In order to fully understand the roles of defects as the active sites of adsorption, the PL spectra of CVD and ME MoS_2 sample were measured in air and vacuum, respectively. Surprisingly, as shown in Figure 4(a), the PL intensity of CVD grown 1L MoS_2 decreased dramatically when measured in vacuum. At the same time, the emission intensities are reversible when exposed in

DISTRIBUTION A: Approved for public release: distributuion unlimited

air again. However, for the PL spectra of ME sample (Figure 4(b)), the intensities don't show obvious variations. The decreased PL intensity of CVD sample in higher vacuum level implies the adsorbates adsorbed on the surface of MoS_2 highly affect its PL intensity. It is noted that the more adsorbates, the stronger of PL intensity. Moreover, it is found that in Figure 4(c), the ratio of PL intensities between CVD and ME MoS_2 samples is even less than 1 when the adsorbates level is low in samples at higher vacuum level ($1x10^{-5}$ mbar). This result shows that the PL intensity of CVD samples is comparable or weaker than that of ME sample, which verifies that the room-temperature optical performance doesn't directly relate to crystal quality. Figure 4(d) demonstrates the vacuum level dependent the ratios of emission intensities of exciton and trion, since it is well known that both of exciton and trion emission evolved in PL spectra. It is observed that the emission intensities of exciton highly depend on the vacuum level, while trion emission is not sensitive to the ambient.

With its moderate band gap size, phosphorene can be switched between insulating and conducting states, and it is still flat enough to confine electrons so that charge flows quickly, leading to a high carrier mobility that is prized by electrical engineers. Our initial investigations on the phosphorene IR photo-detector will mostly rely on the mechanical method for preparing the channel material (See Figure 3(c, d) for our preliminary experimental result). However, it is not easy to use such method for controlled patterning. Moreover, it is neither efficient nor scalable for practical applications. Therefore, it is highly valuable to develop a controllable, efficient and scalable alternative method for the fabrication of phosphorene, which will be crucial for making any phosphorene-based new devices appealing to the commercial market. Our research group has rich experience in synthesizing various high quality low-dimensional materials, including carbon nanotubes, graphene, transitional metal dichalcogenides, etc. [Yang2013, Shi2013, Shi2012] We shall explore new and superior fabrication methods for phosphorene, in order to pave the way to its industrial productions. Furthermore, we shall develop methods for controlling nanoscale patterning in phosphorene samples. This will be important for optimizing the resulting photo-detector's performance. The rich variety of properties that 2D layered material systems offer can potentially be engineered on-demand, and they create exciting prospects for device and technological applications in the proposed field. Reports exist of non-graphene 2D atomic layers integrated into devices which exhibit exceptional performance; for example, one research groups in the US [Geim2013] reported 2D materials based transistors (i.e., monolayer MoS_2) could have ON/OFF ratios more than 3 orders of magnitude higher than the best graphene transistors. The synthesis of atomic layers by vapor phase deposition methods have also emerged recently, which we have successfully demonstrated in SUTD research labs very recently. A variety of studies on the synthesis, chemical modification methods, device fabrication and testing, and theoretical exploration of structure-property correlations are also undergoing based on different 2D atomic layered materials systems. Therefore, it is timely and important to start this proposed research to explore this cutting-edge research and stimulate technologically significant applications.

DISTRIBUTION A: Approved for public release: distributuion unlimited

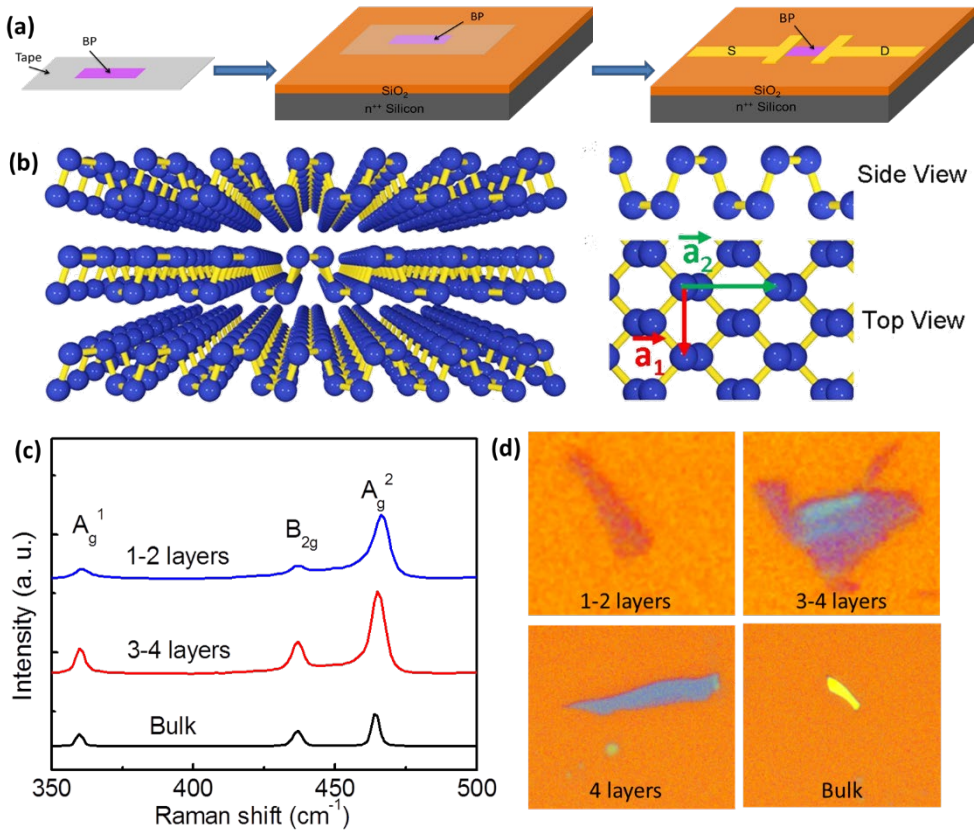

Figure 5. Process of mechanical exfoliation method to fabricate photo-detectors with simple field-effect transistor configuration. S and D represent source and drain electrodes. (b) Few layer and single layer phosphorene structure. (c) Raman spectrum for the phosphorene samples with different number of layers. (d) Optical image of a 2D phosphorene nanosheet on SiO_2 substrate.

After the phosphorene sample is prepared and fully characterized by various state-of-the-art characterization equipment in our research lab such as atomic force microscopy (AFM), transmission electron microscopy (TEM), Raman spectroscopy, X-ray photoelectron spectroscopy etc., we shall construct a prototype two-terminal photo-detector device as shown in Figure 3(a). It has a field effect transistor structure, and can be fabricated using standard microelectronics fabrication techniques such as e-beam lithography, metal deposition, and lift-off. We shall first investigate the transport properties of the device in the dark state, i.e. without incoming light, follow by shine periodically-modulated light on the device with different light frequency, power, and duration, and measure the photo-current response under a small bias voltage. Important characteristics to extract include the responsivity, the response time, and the detection frequency range. Theoretical analysis and extensive numerical simulations will be carried out to model the photo-carrier generation and transport process in the device based on realistic electronic band structure information. The result will be compared with experiment and further

DISTRIBUTION A: Approved for public release: distributuion unlimited

guide the experiment for improving the device performance by optimizing its configuration. Afterward, the same strategy will be used to realize a simple photodetector based on single layer MoS_2/Phosphorene heterostructures (see Figure 4).

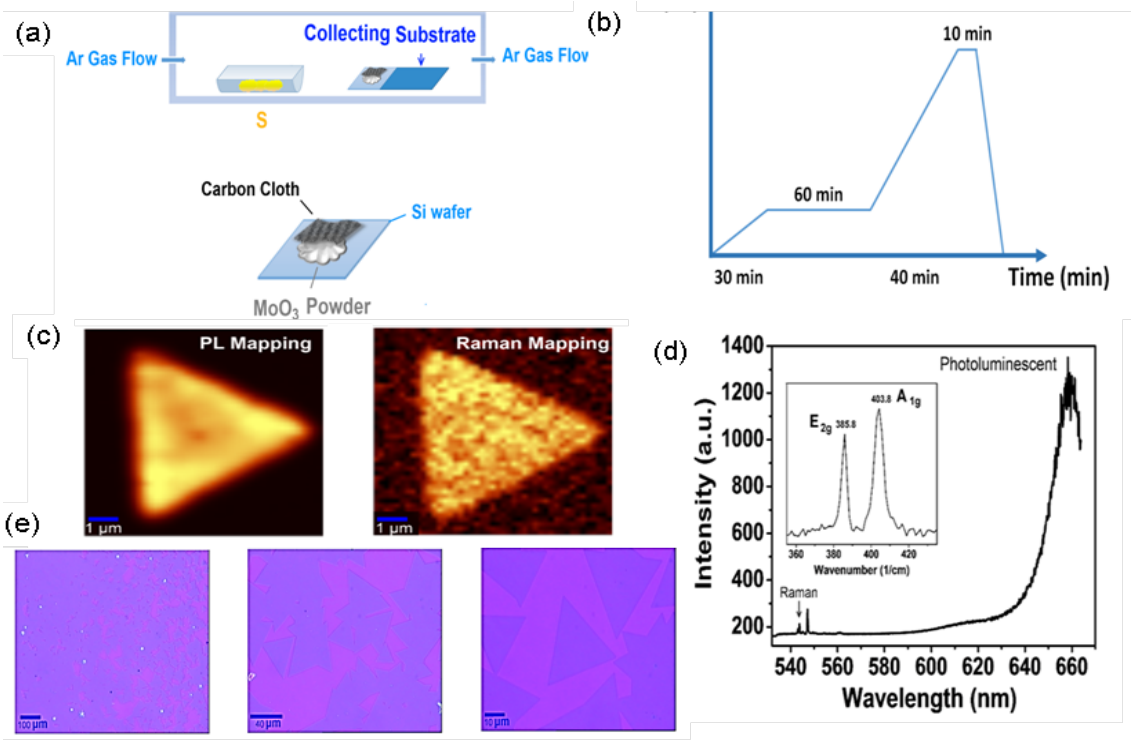

Figure 6. Our preliminary work on fabricating MoS_2 heterostructure based photo-detectors. (a, b) Schematic figure showing the fabrication process. (c,e) The fabricated sample image. (d) Measured photoluminescence spectrum.

Summary

In summary, we demonstrate the possibility of batch production of monolayer MoS_2 and its derivatives grown by CVD technique, as well as the concurrent synthesis technique for the growth of different atomically layered materials. The Raman and PL mappings show the high quality of samples without defects at the edge sites. The STEM and diffraction data show the high crystal quality. The electrical performance of CVD grown monolayer MoS_2 by this technique is comparable to that of mechanically exfoliated samples. Although the common expectation that CVD grown MoS_2 should be structurally defective due to thermal stresses during the growth process, the large mobility of our samples is achieved at 64 cm^2/V-s (RT). Our works indicate the promising future for the implementation of batch production of monolayer MoS_2, its derivatives, and the concurrent synthesis techniques in standard state-of-the-art CMOS fabrication technology. Additionally, we attribute the strong PL intensity to the p doping effects of adsorbates at the defect-sites of CVD samples and its PL intensities will decrease significantly when measured in vacuum. The CVD samples under different grown conditions are expected with different crystal

DISTRIBUTION A: Approved for public release: distributuion unlimited

qualities, which show the decreasing of PL intensities in vacuum by different extent which further confirm the observed phenomenon. The first principle calculations are carried out to investigate the charge transfer process between MoS_2 and adsorbates and further clarify the p-doping effect of adsorbates due to the strong electronegativity of adsorbates. Such a p-doping effect from adsorbates perfectly reduces the concentration of excess electron in MoS_2 and contributes to the radiative process of exciton. This work differs from yet complements previous reports and can guide the future work on the engineering of PL emission intensity on monolayer two dimensional layered semiconductor materials.

DISTRIBUTION A: Approved for public release: distributuion unlimited